NACA

RESEARCH MEMORANDUM

AN INVESTIGATION OF THE CHARACTERISTICS OF AN UNSWEPT WING OF ASPECT RATIO 4.01 IN THE LANGLEY 8-FOOT HIGH-SPEED TUNNEL

By Ralph P. Bielat and Maurice S. Cahn

Langley Aeronautical Laboratory
Langley Air Force Base, Va.

NATIONAL ADVISORY COMMITTEE FOR AERONAUTICS

WASHINGTON
November 8, 1949

NATIONAL ADVISORY COMMITTEE FOR AERONAUTICS

RESEARCH MEMORANDUM

AN INVESTIGATION OF THE CHARACTERISTICS OF AN UNSWEPT WING OF ASPECT RATIO 4.01 IN THE LANGLEY 8-FOOT HIGH-SPEED TUNNEL

By Ralph P. Bielat and Maurice S. Cahn

SUMMARY

An investigation of the characteristics of a low-aspect-ratio wing was conducted at high subsonic Mach numbers in the Langley 8-foot high-speed tunnel. The wing model had an NACA 65-108 airfoil section, an aspect ratio of 4.01, a taper ratio of 0.498, and no twist or dihedral. The results of the investigation indicated that the severe changes in aerodynamic characteristics usually associated with wings of average or high aspect ratio were alleviated to a great extent by employing a wing of aspect ratio 4.01. The abrupt decrease in lift-curve slope and change in angle of zero lift when compared with a wing of aspect ratio 9.0 and the wings of NACA TN 1665 were less pronounced and were delayed to higher Mach numbers. As the Mach number increased from 0.40 to 0.90 the aerodynamic-center location for the wing of aspect ratio 4.01 moved rearward 7 percent as compared with a rearward movement of 12 percent for the wing of aspect ratio 9.0. The Mach number at which the drag begins to increase rapidly was delayed to a value which was approximately 0.07 higher than that for the wing of aspect ratio 9.0.

INTRODUCTION

Numerous investigations have indicated that flight with airplanes of conventional design in the high subsonic or transonic region would prove to be extremely difficult because of the changes in aerodynamic characteristics of the airplane associated with the flow changes over the wing in the supercritical speed range. These changes, reported both from flight and wind-tunnel data, have been observed as large drag increases, severe increases in longitudinal stability, losses in control effectiveness, and buffeting of the horizontal tail.

Investigations made in this country and in Germany have shown that the speeds at which the adverse effects occurred could be delayed to high subsonic values by use of wings having large amounts of sweepback or sweepforward. A recent investigation (reference 1) has shown that wings of small aspect ratio could also be used to delay the speeds at which the adverse effects occurred. The results of this investigation indicated that improvements in the aerodynamic characteristics of low-aspect-ratio wings in the supercritical speed range were a result of the three-dimensional relieving effects at the tips. These data, however, were obtained for wings employing NACA 0012 airfoil sections with rectangular plan form and having square wing tips. It could be expected that the use of thinner wings employing high-critical-speed sections and with rounded tips would lead to further improvements in delaying the speed at which the adverse effects occurred. The purpose of this report, therefore, is to present data for a wing of low aspect ratio which utilizes a high-critical-speed section and rounded wing tips and to make comparisons with wings of high aspect ratio.

The results reported herein include data at high subsonic Mach numbers for a wing of aspect ratio 4.01 having an NACA 65-108 airfoil section, a taper ratio of 0.498, and no twist or dihedral. These data were originally obtained in conjunction with a general research program undertaken by the NACA to provide information at high subsonic Mach numbers on the component parts of an airplane. The data as reported in reference 2 were obtained specifically for a horizontal-tail model. The data as presented herein include the data of reference 2 for the model with zero control deflection plus wake-survey measurements which were not previously reported.

SYMBOLS

The symbols and aerodynamic coefficients used in this report are defined as follows:

A aspect ratio

a speed of sound in undisturbed stream

b span of model

c section chord of wing

$\bar{c}$ mean aerodynamic chord of wing

M Mach number (V/a)

p	static pressure in undisturbed stream
p_l	local static pressure at point on airfoil section
P	pressure coefficient $\left(\frac{p_l - p}{q}\right)$
P_{cr}	pressure coefficient corresponding to attainment of local speed of sound at some point on airfoil section
q	dynamic pressure in undisturbed stream $\left(\frac{1}{2}\rho V^2\right)$
R	Reynolds number $\left(\frac{\rho V \bar{c}}{\mu}\right)$
S	area of wing
V	velocity in undisturbed stream
x	distance along chord from leading edge of airfoil section
y	distance along semispan from center line
α	angle of attack
ρ	mass density in undisturbed stream
μ	coefficient of viscosity in undisturbed stream
c_n	wing section normal-force coefficient $\left(\frac{1}{c}\int_0^c (P_L - P_U)dx\right)$
c_m	wing section pitching-moment coefficient about 25-percent-chord station $\left(\frac{1}{c^2}\int_0^c (P_U - P_L)\left(x - \frac{c}{4}\right)dx\right)$
C_N	wing normal-force coefficient $\left(\frac{2}{S}\int_0^{\frac{b}{2}} c_n c \, dy\right)$
$C_{m_{\bar{c}/4}}$	wing pitching-moment coefficient about 25-percent-chord station of mean aerodynamic chord $\left(\frac{2}{S\bar{c}}\int_0^{\frac{b}{2}} c_m c^2 dy\right)$

a_n slope of wing section normal-force curve per-degree $\left(\frac{dc_n}{d\alpha}\right)$

ΔH loss of total pressure in wake

c_{d_o} wing section profile-drag coefficient from wake-survey measurements

C_{D_o} wing profile-drag coefficient $\left(\frac{2}{S}\int_0^{\frac{b}{2}} c_{d_o} c\ dy\right)$

Subscripts:

fb force break

L lower surface of airfoil section

U upper surface of airfoil section

APPARATUS AND METHODS

The Langley 8-foot high-speed tunnel, in which the tests were conducted, is of the single-return, closed-throat type.

Model.- The wing model tested had a modified NACA 65-108 airfoil section, an aspect ratio of 4.01, a taper ratio of 0.498, and no twist or dihedral. The 70-percent-chord line was used as the reference station in the design of the wing and the quarter-chord line, as a result, was swept back approximately 8.64°. The wing was originally designed for use as a horizontal-tail model (reference 2) and therefore was equipped with elevators and trim tabs. The NACA 65-108 airfoil section from the 70-percent-chord station to the trailing edge was modified to make the sides of the elevators and trim tabs straight. The ordinates for the NACA 65-108 airfoil section, as modified, are given in table I, and general dimensions of the wing are shown in figure 1. Dimensions for the tip shape of the wing model are given in table II.

Twenty static-pressure orifices were placed at each of four spanwise stations in lines perpendicular to the 70-percent-chord station. The spanwise stations at which pressure measurements were taken were located on the left half of the wing at 15, 40, 70, and 90 percent semispan. A detailed description of the wing will be found in reference 2.

Support.- The wing was supported in the tunnel by means of a vertical steel plate which had a modified-ellipse section of 50-inch chord and 0.75-inch maximum thickness. The surfaces of this plate formed reflection planes for the two wing semispans. Additional information about the support plate is to be found in reference 3.

Procedure.- Lift and moment data were obtained from pressure-distribution measurements made at each of the four spanwise stations. The measurements were made for angles of attack from -2° to 6° at Mach numbers varying from 0.40 to 0.925. Drag data were determined by the wake-survey method with a rake located approximately 1.56-root-chord lengths behind the wing 70-percent-chord station. The wake surveys were made at the 15-, 40-, 70-, and 90-percent-semispan stations by means of the rake described in reference 3. The gaps between the stabilizer and elevator were sealed such that the model was aerodynamically smooth for the wake-survey measurements. The drag measurements were taken at 0°, 3°, and 6° angle of attack for Mach numbers of 0.645 to 0.885. The drag data were limited to a maximum Mach number of 0.885 since the tunnel choked at the wake-survey rake support strut. As explained in reference 3, choking at the survey strut imposes a limitation on the maximum test Mach number and does not affect the applicability of the results.

Reynolds number.- The variation of test Reynolds number, based on the mean aerodynamic chord of the wing, with Mach number is presented in figure 2.

Corrections.- Tunnel-wall-interference corrections, using the methods of references 4, 5, 6, and 7, have been applied to the data up to and including a Mach number of 0.90. The magnitude of the corrections was found to be very small; the maximum corrections to the Mach numbers even at a Mach number of 0.90 were approximately 1 percent. The corrections to the coefficients due to corrections in dynamic pressure were also small, the maximum correction being about 2 percent. As brought out in reference 2, the tunnel choked in the present tests at a Mach number of approximately 0.95. Numerous tests have shown that, when choking occurs, the data are no longer comparable to free-air characteristics. There was also a tendency towards choking at a Mach number of 0.925. The results obtained at this Mach number, even if completely corrected for the usual effects of wind-tunnel-wall interference, may not, therefore, indicate free-air characteristics. The data which have been included herein for a Mach number of 0.925 are therefore considered to be of uncertain value.

REDUCTION OF DATA AND RESULTS

In the reduction of the data, the section pressure distributions measured at the four spanwise stations were plotted and then mechanically integrated to obtain section normal-force coefficient c_n and section pitching-moment coefficient c_m. The section coefficients were then used to make plots of $c_n c \frac{b}{S}$ and $c_m c^2 \frac{b^2}{S^2}$ against the semispan stations which were mechanically integrated to give the wing normal-force coefficient C_N and wing pitching-moment coefficient $C_{m_{\bar{c}/4}}$, respectively. Typical plots of the pressure distributions for two spanwise stations which were used to obtain the wing section coefficients are shown in figure 3.

The total-pressure and static-pressure measurements made during the wake surveys have been reduced to section profile-drag coefficients using the methods given in reference 8. The wing profile-drag coefficient was then obtained from mechanical integration of curves of $c_{d_o}c$ against the semispan.

The variations of wing normal-force, wing pitching-moment, and wing profile-drag coefficients with Mach number for several angles of attack are presented in figure 4 while figure 5 shows the variations of angle of attack, wing pitching-moment, and wing profile-drag coefficients plotted against wing normal-force coefficient. The variations of section normal-force coefficient with Mach number at two spanwise stations for angles of attack of 2° and 6° are shown in figure 6. The effect of Mach number on the section normal-force-curve slopes at two spanwise stations is presented in figure 7. The slopes of the curves were measured between 0° and 3° angle of attack. Figure 8 shows the change in aerodynamic-center location with Mach number. The aerodynamic-center location was determined for a wing normal-force coefficient of 0.2. Figure 9 presents the variation of section profile-drag coefficient with Mach number at two spanwise stations for section normal-force coefficients of 0 and 0.5. The variation of drag coefficient with Mach number for a wing loading of 60 pounds per square foot at an altitude of 35,000 feet, including the calculated induced drag, is shown in figure 10. Figure 11 shows the variation of force-break Mach number with aspect ratio as computed by the methods of reference 9. The force-break Mach number is estimated roughly as the Mach number for which the drag coefficient first begins to rise rapidly.

Spanwise variations of section loadings, section moments, and section drags from which the wing characteristics were determined are shown in figures 12, 13, and 14, respectively. These figures can be utilized in determining the bending and twisting moments that occur on the wing.

Figure 15 presents the losses of total pressure in the wake behind the wing for four spanwise stations for Mach numbers of 0.645, 0.822, and 0.885.

DISCUSSION

Normal-Force Characteristics

In general, there were no serious changes in the wing normal-force characteristics below a Mach number of 0.86 for the angle-of-attack range investigated (fig. 4). It can be seen in figure 5 that the angle for zero lift remained fairly constant up to a Mach number of approximately 0.86 and then shifted positively at supercritical Mach numbers. The shift in angle for zero lift in the range of Mach numbers from 0.86 to 0.905, however, amounted to approximately 0.6°. Similar effects were noted for the low-aspect-ratio wings reported in reference 1. On the other hand, the data of reference 1 for the high-aspect-ratio wings and the data of reference 3 for a wing of aspect ratio 9.0 indicated large and erratic changes in the normal-force characteristics at supercritical Mach numbers.

The section normal-force characteristics at two spanwise stations for the wing are shown in figure 6, together with the section characteristics for the wing of reference 3 which employs an NACA 65-210 airfoil section and which has an aspect ratio of 9.0. The data for the wing of aspect ratio 9.0 have been plotted for angles of attack which would very nearly give values of the section normal-force coefficient in the subcritical region comparable to those of the present wing. It can be seen that the usual increase in section lift in the supercritical range, as well as the abrupt decrease in the supercritical range, was much lower for the low-aspect-ratio wing as compared with the high-aspect-ratio wing, particularly at the inboard station and high angle-of-attack condition. Similar effects are to be noted for the section normal-force-curve slopes shown in figure 7. The increase in the normal-force-curve slope with Mach number, as well as the abrupt decrease of slope at supercritical Mach numbers, for the low-aspect-ratio wing was less than that for the wing of aspect ratio 9.0. The Mach number at which the slope "breaks" (decreases) for the wing of the present investigation was approximately 0.875 as compared with a Mach number of 0.76 for the aspect ratio 9.0 wing. This represents an increase of 15 percent in the "force-break" Mach number. Since the wing of aspect ratio 9.0 has an airfoil section which has more camber and thickness than the wing in the present investigation, the improvement in the aerodynamic characteristics for the wing of aspect ratio 4.01 is not due entirely to the reduction in aspect ratio. Approximate calculations indicate that the combined effects of decrease in camber and thickness for the NACA 65-108 airfoil result in an approximately 7-percent increase in the critical speed of that of the NACA 65-210 airfoil and therefore the remaining 8 percent is due presumably to the reduced aspect ratio.

The theoretical work done in reference 9, which considers the flow about a series of thin ellipsoids, further substantiates the improvements which can be gained in the critical speed by use of ellipsoids of low aspect ratio. The theory, however, indicates only qualitative agreement since the theory underestimates the experimental results quantitatively. It is seen in figure 6 that, when the section characteristics at the 40-percent-semispan and 90-percent-semispan stations are compared, the three-dimensional relieving effects of the tip are greater for the low-aspect-ratio wing than for the wing of aspect ratio 9.0. A further example of the relieving effects of the tip on the spanwise section characteristics for the two wings can be seen in figure 12. The data are compared for angles of attack which give approximately the same section normal-force coefficient at subcritical Mach numbers. Careful observation indicates that there was very little spanwise movement of the lateral center of load for the wing of aspect ratio 4.01 through the Mach number range. On the other hand, it can be seen that there were large outboard shifts in the lateral center of load on the wing of aspect ratio 9.0 at supercritical Mach numbers. It was shown in reference 3 that these shifts were due primarily to the fact that the lift losses at the tip were less severe than those at any of the inboard sections because of the effect of tip relief. It was also shown quantitatively in reference 9 that the three-dimensional relief increased with a decrease in the aspect ratio, especially at high Mach numbers. As a result of the tip-relieving effects, therefore, it could be expected that the wing of aspect ratio 4.01 would undergo less severe spanwise variations in section characteristics.

It was stated in reference 1 that further improvements in the aerodynamic characteristics of low-aspect-ratio wings could be expected by employing wings of thin sections and late-critical-speed types and which had suitably shaped tips. A comparison of the lift-curve slope for a wing of aspect ratio 4, obtained by interpolation of the data from reference 1, with the lift-curve slope for the present wing of aspect ratio 4.01 indicates that the Mach number for the lift-curve "break" is increased by 0.08 for the present wing. This represents an approximate 10-percent increase in the "force-break" Mach number for the present wing over that of the wing of reference 1 which has an NACA 0012 airfoil section and which has a rectangular plan form and square wing tips.

Pitching-Moment Characteristics

At angles of attack near 0°, the variation of pitching-moment coefficient with Mach number indicated gradual negative increases in the subcritical speed range, whereas the pitching-moment coefficients for 4° and 6° angle of attack showed gradual positive increases (fig. 4). As the Mach number was increased to supercritical values, the pitching moments indicated rather large diving tendencies. The variation of the moments with angle of attack was reversed such that the slopes became stable. Figure 5 shows the pitching-moment coefficients plotted against normal-force coefficient for several Mach numbers. This figure clearly indicates the change in pitching-moment slope from positive to negative values as the Mach number was increased above 0.85. These changes in pitching moment have been shown in several investigations and from schlieren photographs to be associated with movement of the shock on the upper and lower surfaces of the wing.

The effect of Mach number on the aerodynamic-center location, expressed in percent of the mean aerodynamic chord, is given in figure 8. It can be seen that the aerodynamic center is located forward of the quarter-chord point for Mach numbers below 0.85. Above a Mach number of 0.85 the aerodynamic center moved rearward of the quarter chord such that at a Mach number of 0.90 the aerodynamic center is located at the 29-percent-chord point. This represents an over-all rearward shift of 7 percent in the aerodynamic center as the Mach number increased from 0.40 to 0.90. The aerodynamic-center characteristics for the wing of aspect ratio 9.0 of reference 3 are also included in figure 8 for comparison. The aerodynamic-center location for this wing gradually moved rearward from the quarter-chord station up to a Mach number of 0.825 and then shifted to approximately the 37-percent-chord location as the Mach number increased to 0.90. The changes in the aerodynamic-center location at supercritical Mach numbers are associated with the changes in the chordwise loadings. (See, for instance, fig. 3.) The changes in the aerodynamic-center location coupled with the changes in lift-curve slope and angle for zero lift are the principal causes of the adverse stability changes that occur in the supercritical flight range. Because these changes have been observed to be less severe for the wing of aspect ratio 4.01, it could be expected that flight in the transonic speed range could be made possible with an aircraft employing a low-aspect-ratio wing.

Drag Characteristics

The wing profile-drag coefficients exhibited no unusual characteristics below the Mach number for the abrupt drag rise. The wing profile-drag coefficient at an angle of attack of 0° commenced to increase rapidly when the Mach number was raised above 0.85 (fig. 4). The high Mach number attained before this drag rise occurred is due in part to the low aspect ratio and to the small thickness ratio of the wing.

The section profile-drag characteristics at two spanwise stations for section normal-force coefficients of 0 and 0.5 for the present wing are compared in figure 9 with those of the wing of aspect ratio 9.0. The effects of the reduced aspect ratio, including the combined effects of the reduced camber and thickness on the section profile drag for the present wing, are immediately apparent. It can be seen that the section profile-drag coefficients at the inboard stations as compared with stations near the tip were higher and commenced to increase at lower Mach numbers for both wings. The rapid increase in drag at the inboard stations is caused by separation of the flow over the wing due to shocks which are essentially normal to the flow (fig. 15). Of particular interest is the reduction in the drag for both wings at the 90-percent-semispan station at zero section normal-force coefficient and at the 90-percent-semispan station for the wing of aspect ratio 9.0 at 0.5 section normal-force coefficient. This reduction of drag is the result of the three-dimensional type of flow at the tips. The drag data at the 90-percent-semispan station for the wing of aspect ratio 4.01 at 0.5 section normal-force coefficient is not presented since the flow at this station was associated with tip vortices, thus making the measurements of the drag doubtful. The wake-survey data of figure 15 showed that the losses in the wake at the 90-percent-semispan station at an angle of attack of 6° were characterized by two peaks: one peak located at approximately 1 inch below the chord line representing the direct losses in the wake behind the wing and the other peak representing losses in the flow influenced by the tip vortices.

A comparison of the drags for the wings of aspect ratio 4.01 and 9.0 calculated for a level-flight wing loading of 60 pounds per square foot at an altitude of 35,000 feet (calculated induced drag included) is shown in figure 10. The results indicate that the Mach number at which an airplane using the wing of aspect ratio 4.01 described herein could fly, before large increases of power are required, is increased by approximately 0.07 above that of the wing of aspect ratio 9.0. As to be expected, figure 10 also shows that in the low Mach number range, the drag of the low-aspect-ratio wing is larger than that of the high-aspect-ratio wing because of the higher induced drag. As the Mach number is increased above 0.79 where large increases in power would be first manifested, however, it can be seen that the drag of the low-aspect-ratio wing is considerably smaller. As an example, the lift-drag ratio for the low-aspect-ratio wing is approximately 11.0 at a Mach number of 0.885, whereas the lift-drag ratio for the wing of aspect ratio 9.0 is approximately 4.9. Similar results were observed for the wings of reference 1.

A comparison of the variation of force-break Mach number with aspect ratio for the wing of aspect ratio 4.01 reported herein and the wings of references 1 and 3 are presented in figure 11. It can be seen that reducing the aspect ratio increases the force-break Mach number, especially for the NACA 0012 airfoils. The method of reference 9 has been employed to estimate the effect of reducing the aspect ratio on the force-break Mach number. The theoretical curve for the NACA 65-108 airfoil was obtained by correcting the force-break Mach number of the NACA 65-210 airfoil of aspect ratio 9.0 for the effects of thickness and camber as described previously. It can be seen that very good agreement exists between the theoretical and experimental results for the NACA 65-108 wing at aspect ratio 4.01. Furthermore, it can be seen that the increase in the drag force-break Mach number resulting from a reduction of the aspect ratio from 9.0 to 4.01 amounts to only 1 percent, whereas the increase in the lift force-break Mach number due to a similar reduction in aspect ratio amounts to approximately 8 percent. When this same method is for the NACA 0012 airfoils, however, the correlation between theoretical and experimental data is not good. As explained in reference 9, a quantitative comparison of the experimental results with the theoretical results which considers the flow around a series of thin ellipsoids is not warranted since the wings of reference 1 did not have elliptical sections and plan forms. Qualitatively, however, the results do indicate the improvement which can be obtained by reducing the aspect ratio.

CONCLUSIONS

The results of an investigation of a wing employing an aspect ratio of 4.01, small thickness ratio, and high-critical-speed section indicated the following:

1. In the range of Mach numbers up to 0.86 there were no adverse changes in lift-curve slope and in angle of zero lift. At Mach numbers in the range of 0.86 to 0.90 the changes of the lift-curve slope and angle of zero lift were less severe when compared with a wing of aspect ratio 9.0 or to the wings of NACA TN 1665. The high Mach numbers attained before the lift-curve slope breaks represent an approximate increase of 0.12 and 0.08 in Mach number over that of the wing of aspect ratio 9.0 and the wings of NACA TN 1665, respectively.

2. As the Mach number increased from 0.40 to 0.90 the aerodynamic-center location for the wing of aspect ratio 4.01 moved rearward 7 percent as compared with a rearward movement of 12 percent for the wing of aspect ratio 9.0.

3. The Mach number at which the drag begins to increase rapidly was delayed to a value which was approximately 0.07 higher than that for the wing of aspect ratio 9.0.

Langley Aeronautical Laboratory
National Advisory Committee for Aeronautics
Langley Air Force Base, Va.

REFERENCES

1. Stack, John, and Lindsey, W. F.: Characteristics of Low-Aspect-Ratio Wings at Supercritical Mach Numbers. NACA Rep. 922, 1949.

2. Bielat, Ralph P.: Investigation at High Speeds of a Horizontal-Tail Model in the Langley 8-Foot High-Speed Tunnel. NACA RM L6L10b, 1947.

3. Whitcomb, Richard T.: Investigation of the Characteristics of a High-Aspect-Ratio Wing in the Langley 8-Foot High-Speed Tunnel. NACA RM L6H28a, 1946.

4. Glauert, H.: Wind Tunnel Interference on Wings, Bodies and Airscrews. R. & M. No. 1566, British A.R.C., 1933.

5. Thom, A.: Blockage Corrections in a Closed High-Speed Tunnel. R. & M. No. 2033, British A.R.C., 1943.

6. Goldstein, S., and Young, A. D.: The Linear Perturbation Theory of Compressible Flow, with Applications to Wind-Tunnel Interference. R. & M. No. 1909, British A.R.C., 1943.

7. Allen, H. Julian, and Vincenti, Walter G.: The Wall Interference in a Two-Dimensional-Flow Wind Tunnel with Consideration of the Effect of Compressibility. NACA Rep. 782, 1944.

8. Baals, Donald D., and Mourhess, Mary J.: Numerical Evaluation of the Wake-Survey Equations for Subsonic Flow Including the Effect of Energy Addition. NACA ARR L5H27, 1945.

9. Hess, Robert V., and Gardner, Clifford S.: Study by the Prandtl-Glauert Method of Compressibility Effects and Critical Mach Number for Ellipsoids of Various Aspect Ratios and Thickness Ratios. NACA TN 1792, 1949.

TABLE I

ORDINATES FOR NACA 65-108 AIRFOIL

(Stations and ordinates in percent of wing chord)

Upper surface		Lower surface	
Station	Ordinate	Station	Ordinate
0	0	0	0
.474	.651	.526	-.601
.721	.790	.779	-.720
1.217	.998	1.283	-.890
2.462	1.359	2.537	-1.173
4.959	1.903	5.041	-1.587
7.458	2.330	7.542	-1.906
9.958	2.690	10.042	-2.174
14.960	3.267	15.040	-2.595
19.963	2.710	20.037	-2.914
24.969	4.047	25.031	-3.151
29.974	4.291	30.026	-3.319
34.981	4.453	35.019	-3.423
39.987	4.534	40.013	-3.462
44.994	4.522	45.006	-3.426
50.000	4.409	50.000	-3.305
55.006	4.186	54.994	-3.090
60.011	3.873	59.989	-2.801
65.015	3.486	64.985	-2.456
70.000	3.043	70.000	-2.063
80.000	[a]2.031	80.000	[a]-1.378
90.000	[a]1.016	90.000	[a]-.689
100.000	[a]0	100.000	[a]0

L. E. radius, 0.434
Slope of radius through end of chord, 0.04212

[a]Ordinates derived for straight-side section from 0.70-chord station to trailing edge.

TABLE II

DIMENSIONS OF TIP SHAPE OF WING MODEL IN INCHES

(Symbols defined in fig. 1)

Plan-form contour of tip		
Distance from tip, x	y_s	y_E
0	1.200	-1.200
.010	1.555	-.664
.020	1.697	-.407
.050	1.950	-.080
.080	2.110	.145
.100	2.193	.266
.200	2.493	.678
.300	2.674	.930
.400	2.791	1.083
.500	2.875	1.185
.600	2.932	1.244
.720	2.971	1.273
Elevation contour of tip		
Distance from tip, x	y_U	y_L
0	0	0
.010	.042	.031
.020	.058	.042
.050	.086	.065
.080	.105	.078
.100	.114	.085
.200	.145	.110
.300	.164	.125
.400	.176	.134
.500	.184	.141
.600	.188	.145
.720	.192	.147

NACA

[redacted]

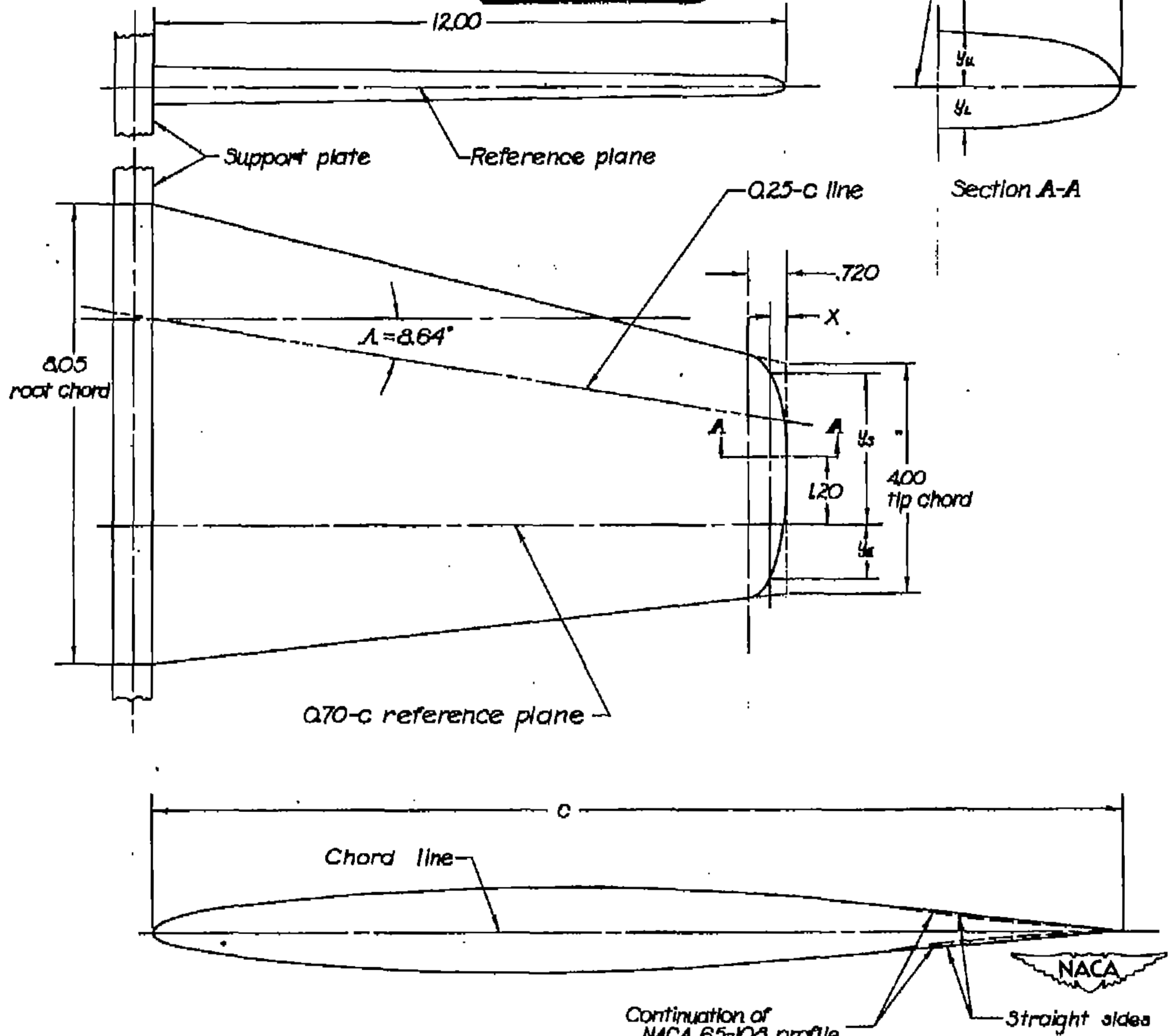

[redacted]

Figure 1.– Details of wing model tested. (Dimensions in inches.)

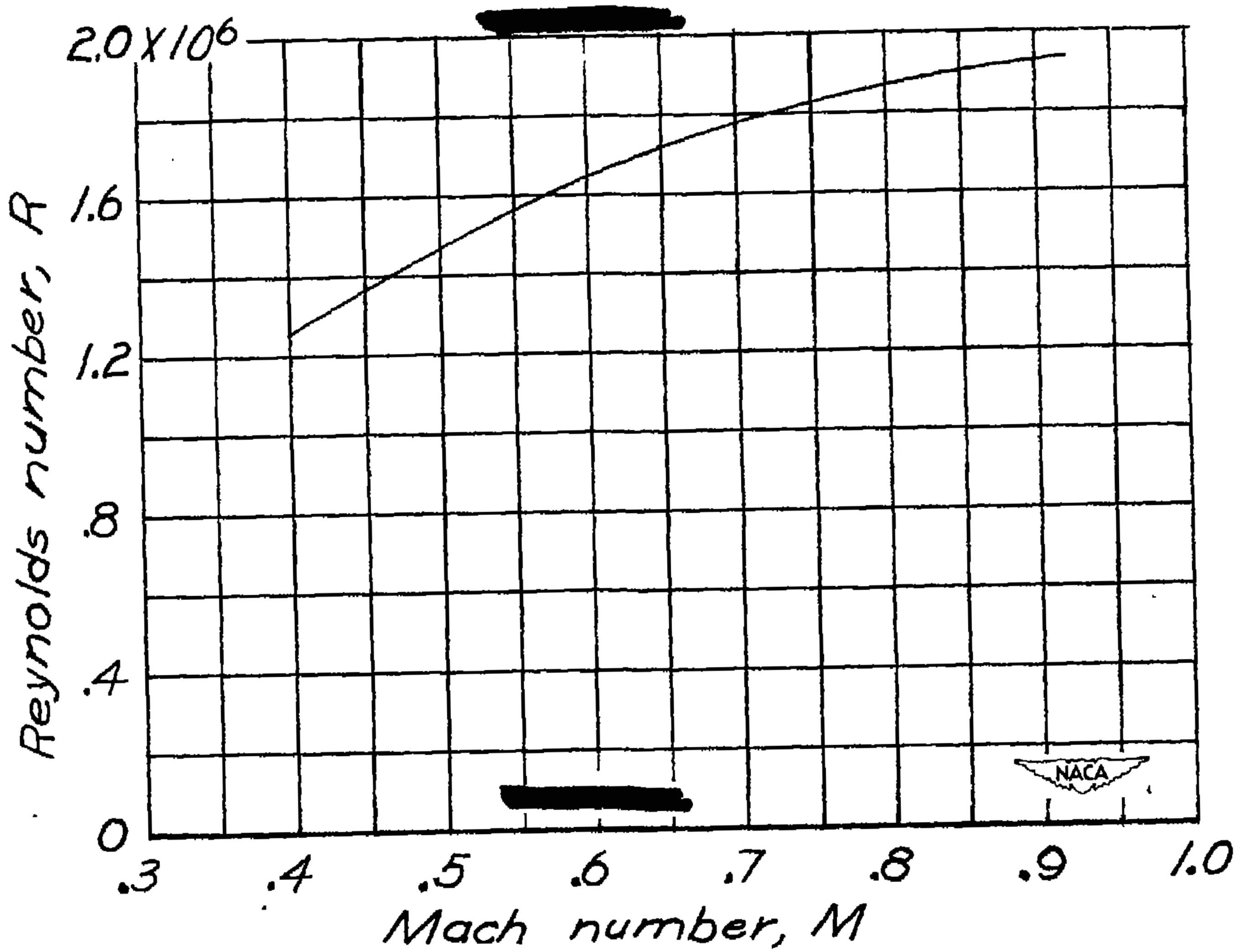

Figure 2.- Variation of Reynolds number with Mach number for the NACA 65-108 airfoil.

[redacted]

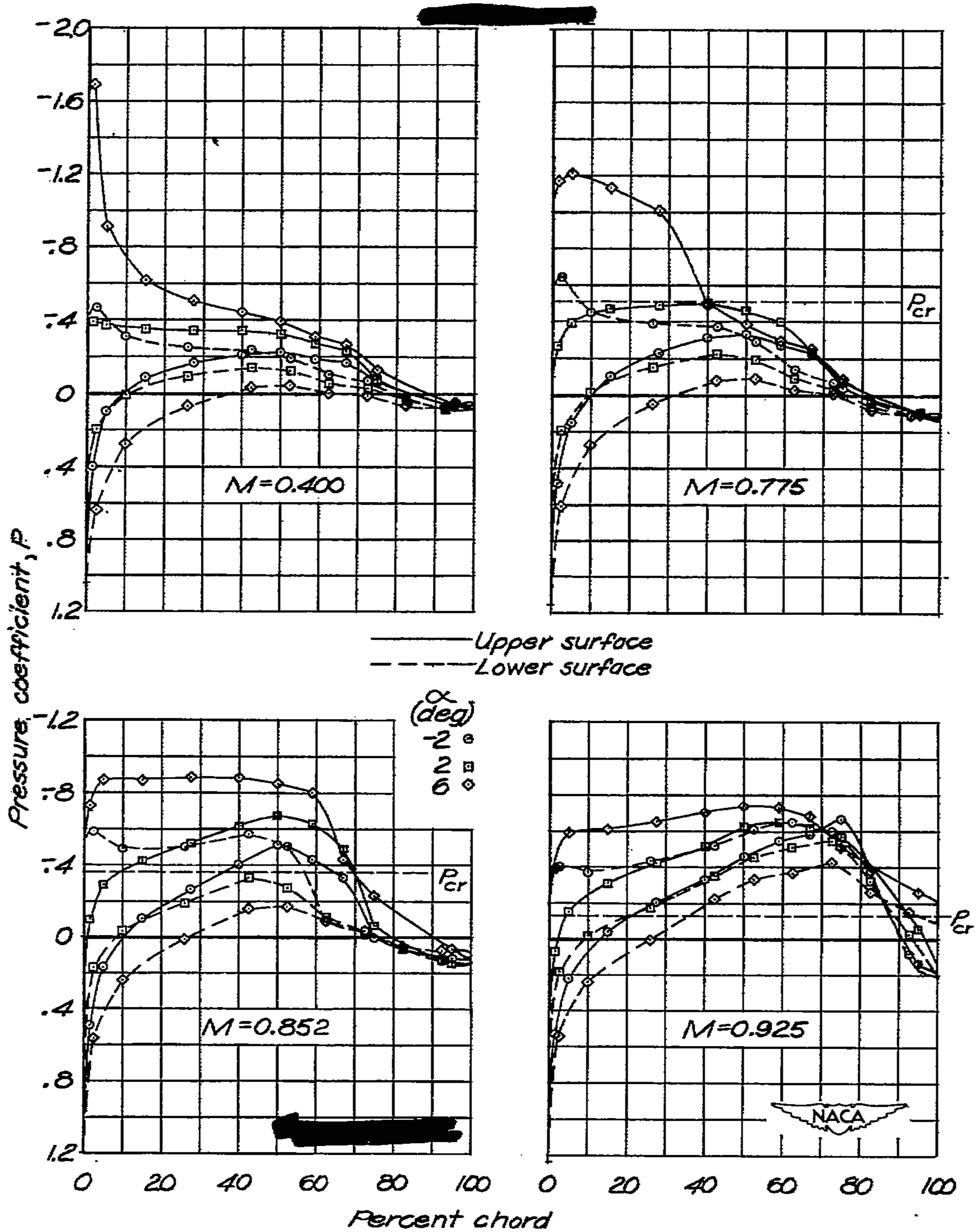

[redacted]

(a) 40-percent-semispan station.

Figure 3.- Pressure distribution about the wing at two semispan stations.

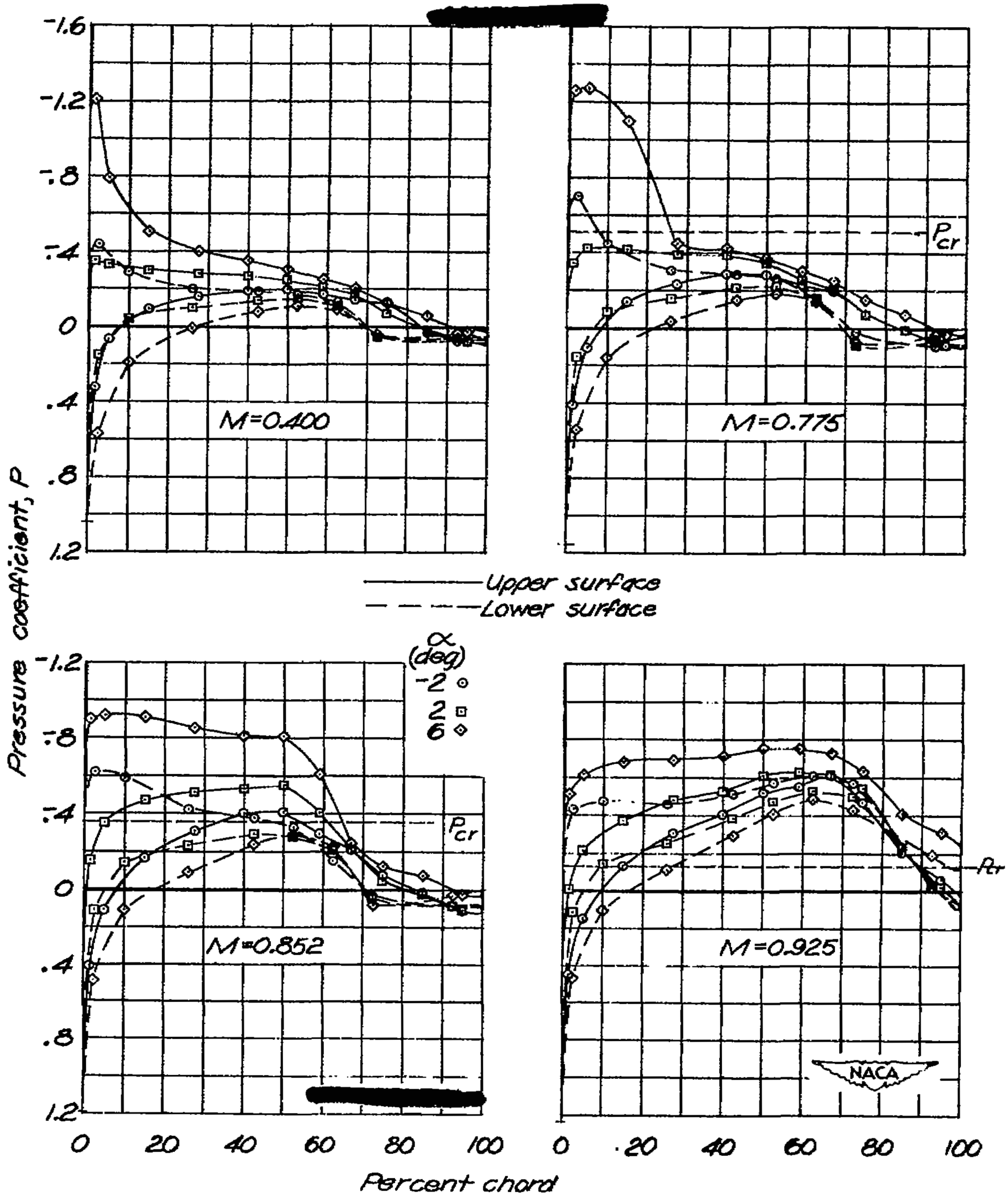

(b) 90-percent-semispan station.

Figure 3.— Concluded.

[redacted]

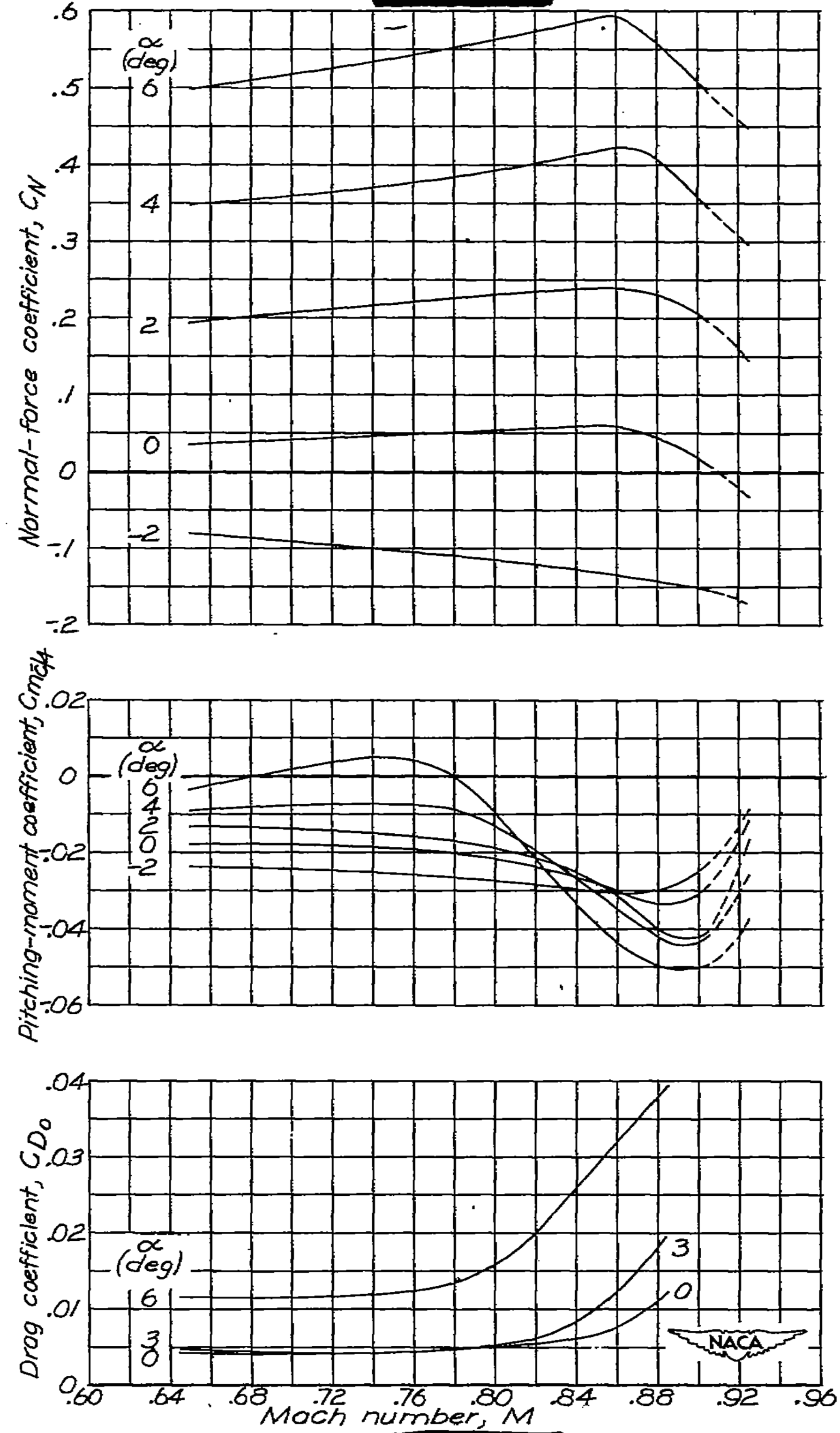

[redacted]

Figure 4.- Variation of wing normal-force, wing pitching-moment, and wing profile-drag coefficients with Mach number.

[redacted]

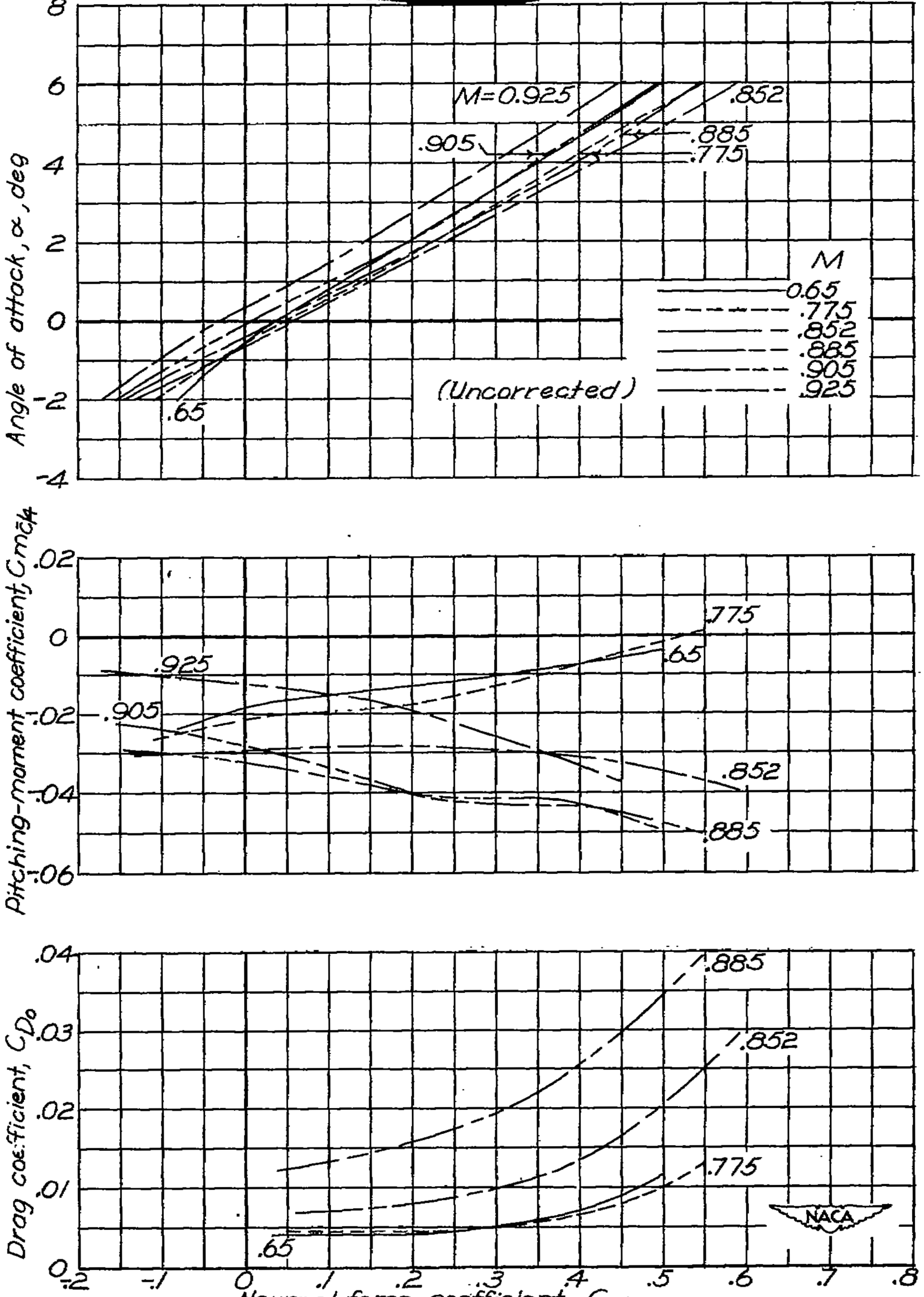

[redacted]

Figure 5.- Variation of angle of attack, wing pitching-moment coefficient, and wing profile-drag coefficient with wing normal-force coefficient.

[redacted]

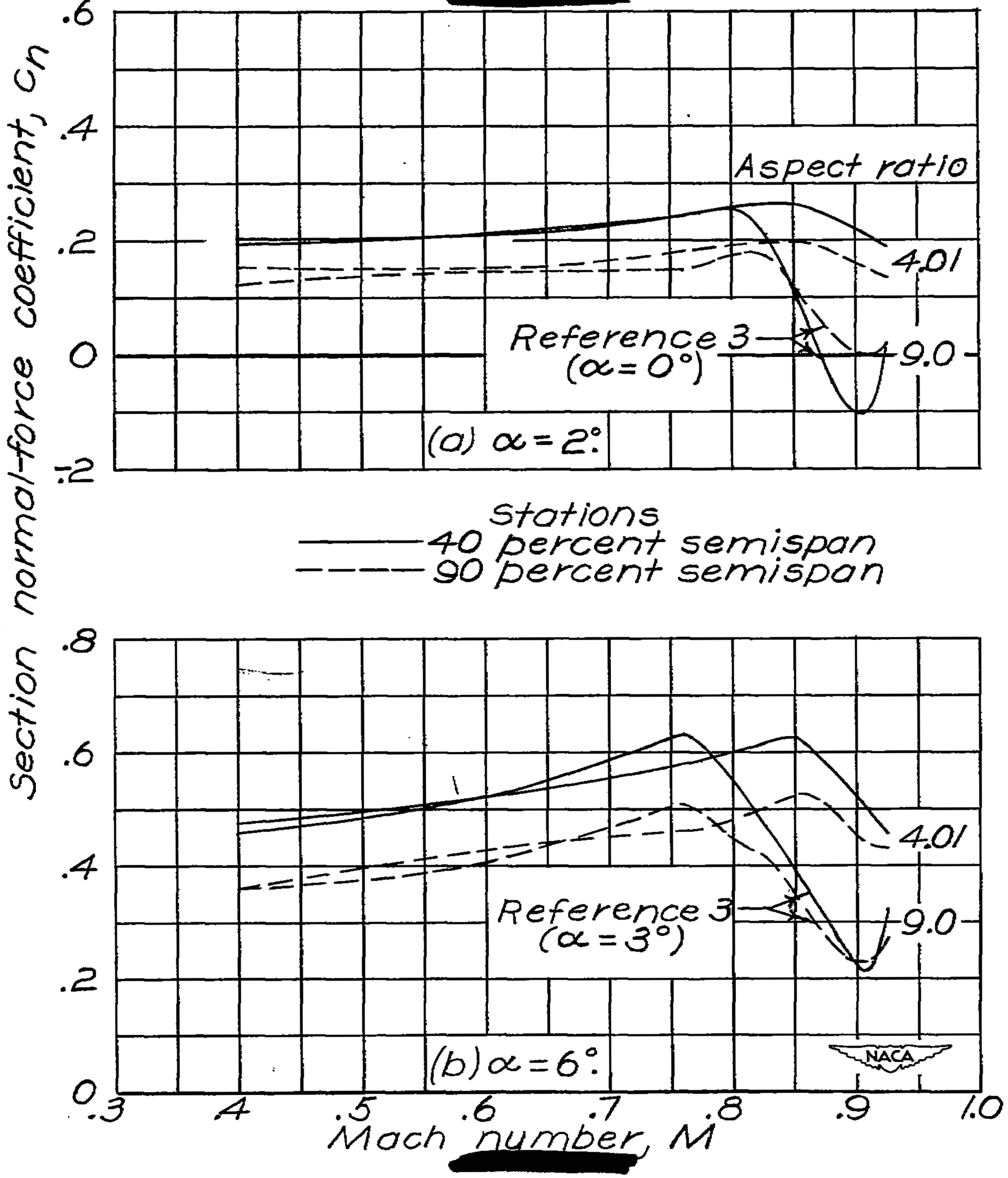

[redacted]

Figure 6.– Variation of section normal-force coefficient with Mach number at two spanwise stations.

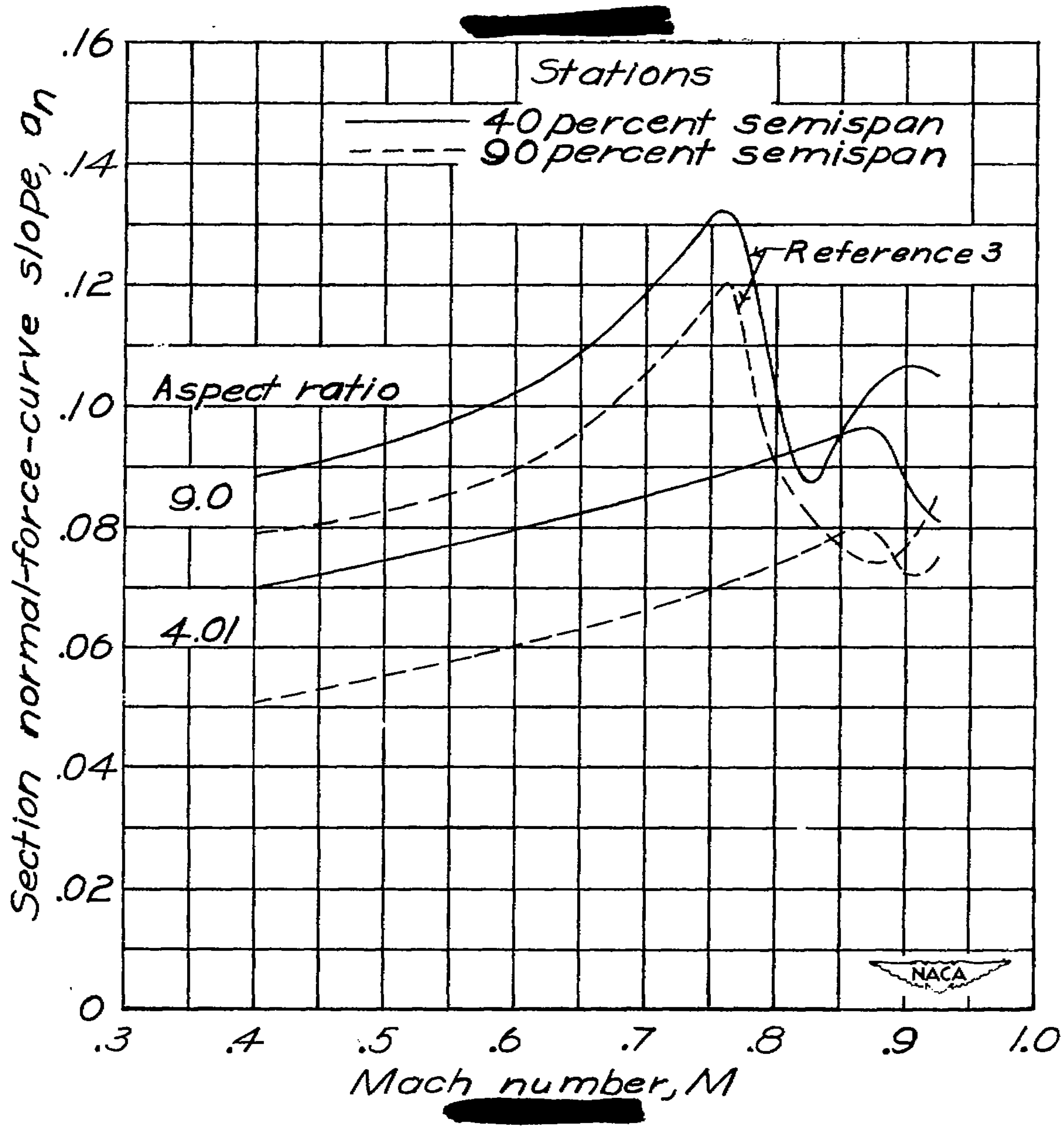

Figure 7.— Variation of section normal-force-curve slope with Mach number.

[redacted]

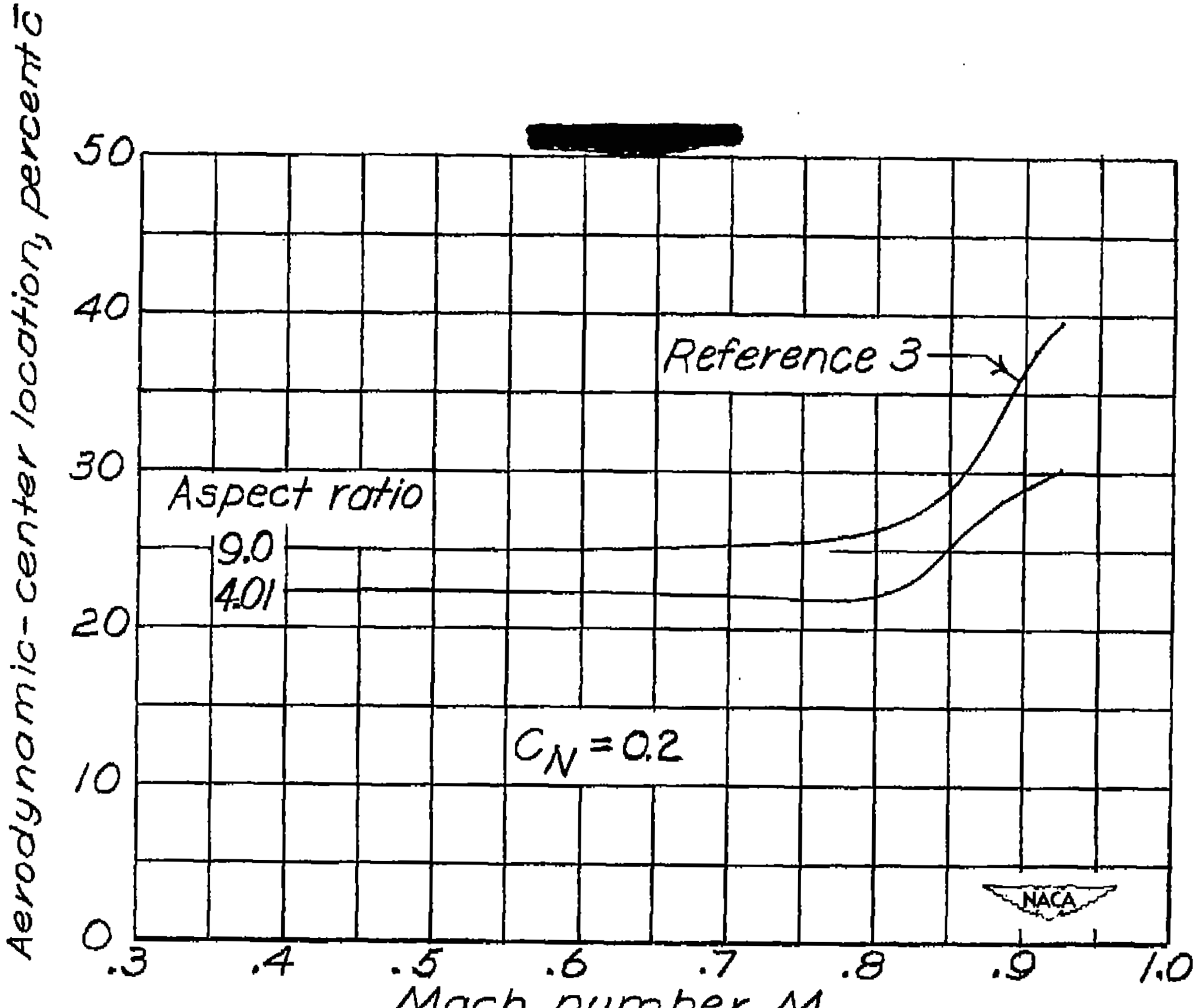

[redacted]

Figure 8.– Variation of aerodynamic-center location with Mach number.

[redacted]

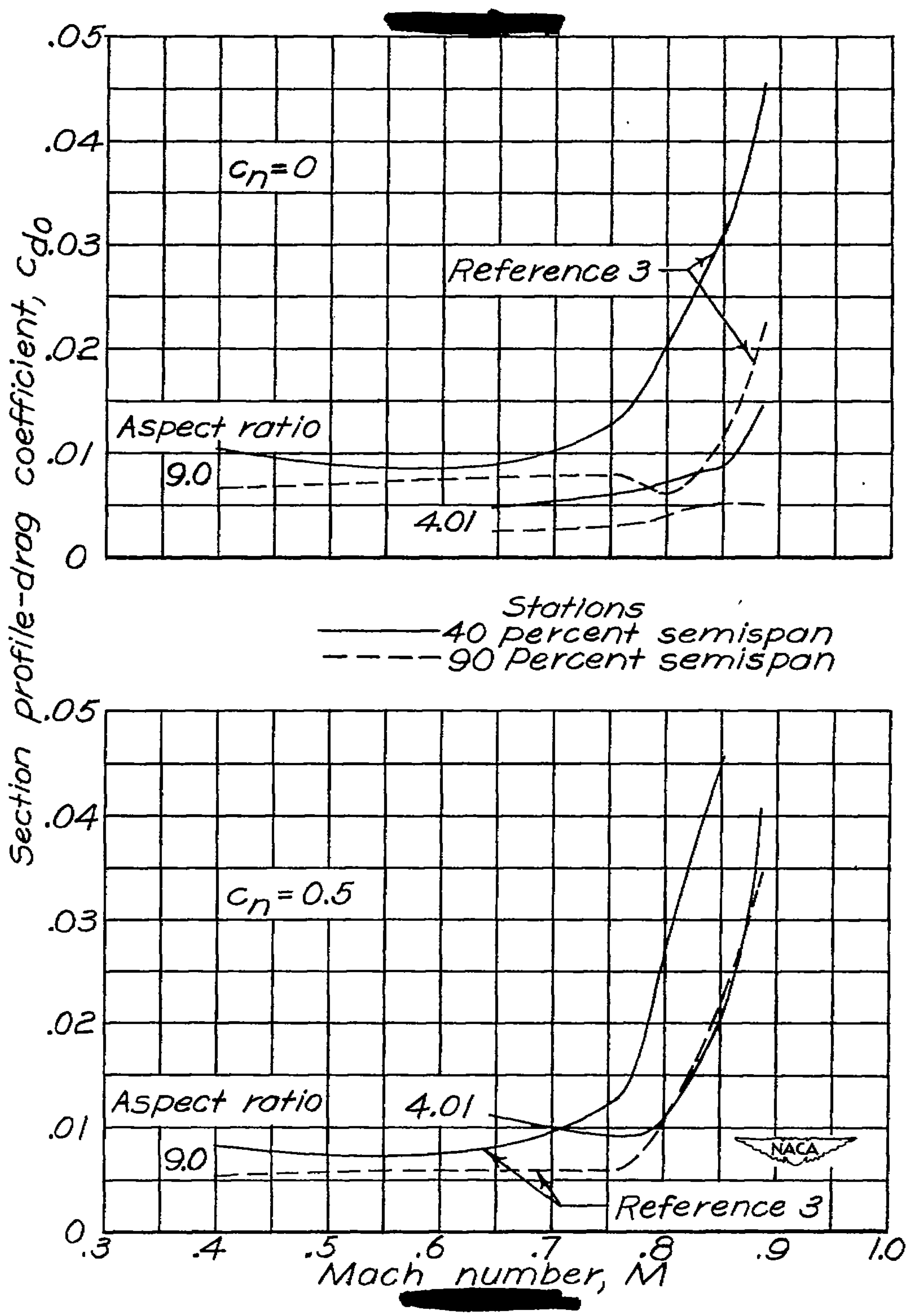

[redacted]

Figure 9.– Variation of section profile-drag coefficient with Mach number at two spanwise stations.

[redacted]

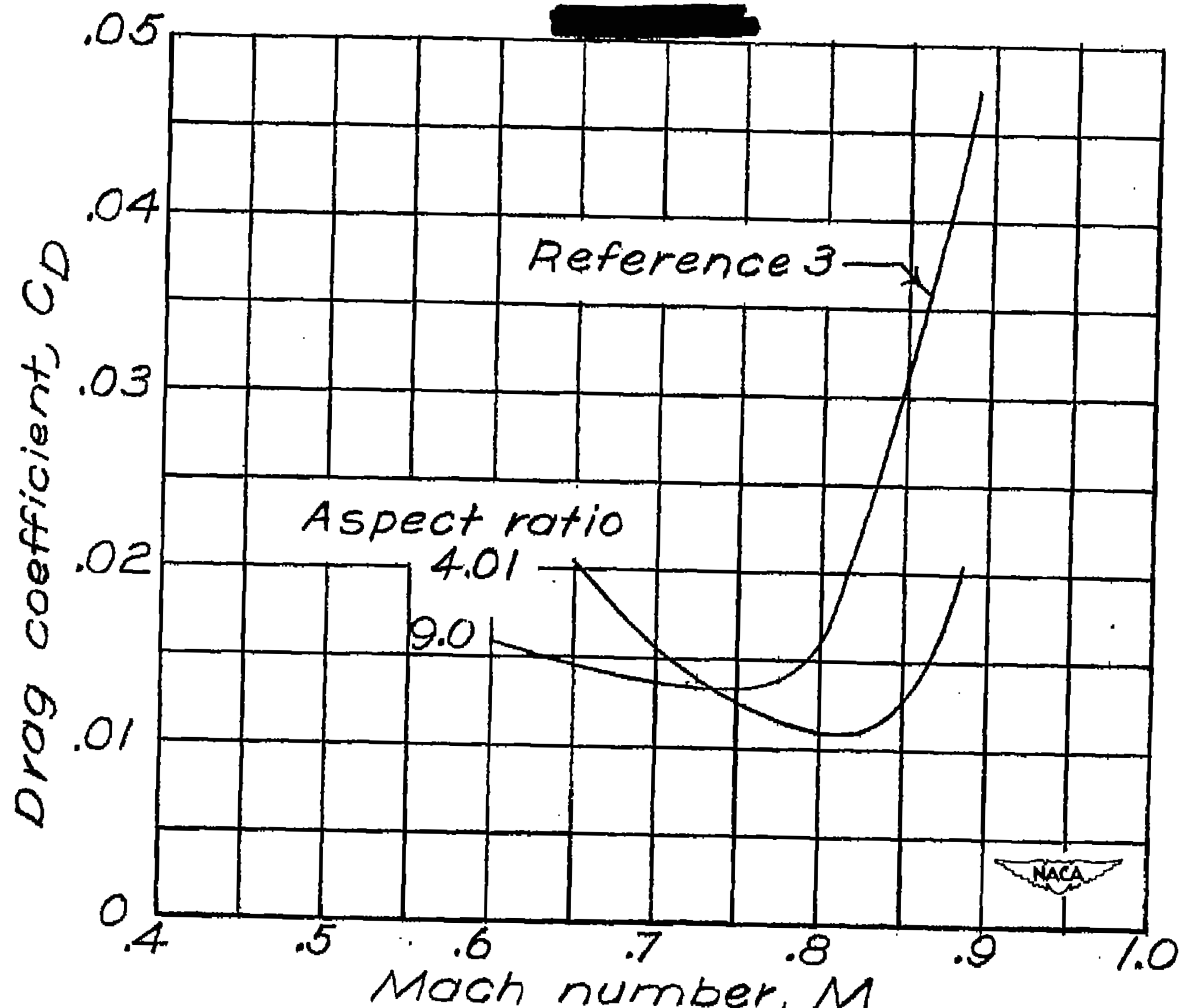

[redacted]

Figure 10.- Variation of drag coefficient with Mach number for wing loading of 60 pounds per square foot at 35,000-foot altitude. (Calculated induced drag included.)

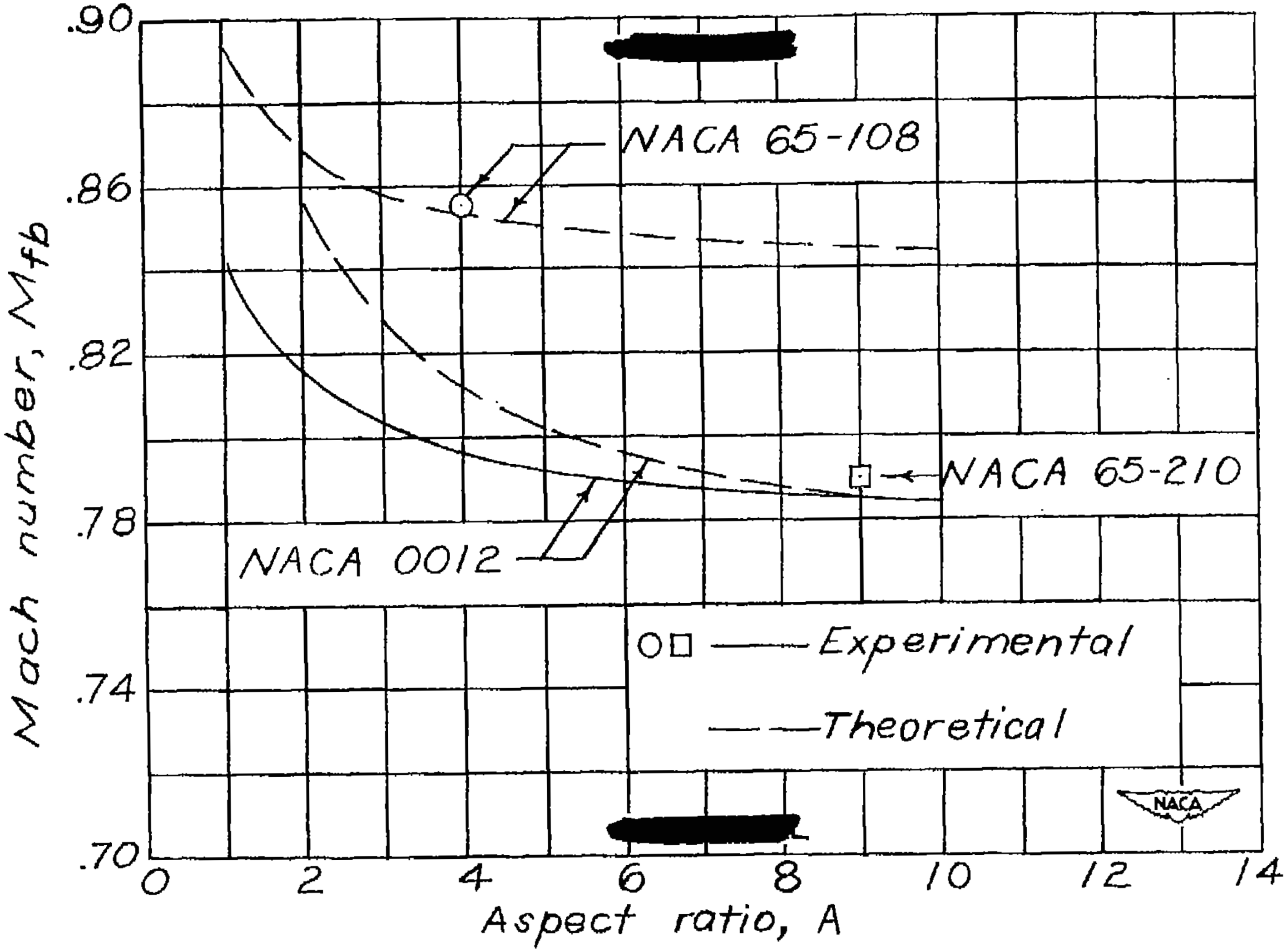

Figure 11.- Variation of force-break Mach number with aspect ratio.

[redacted]

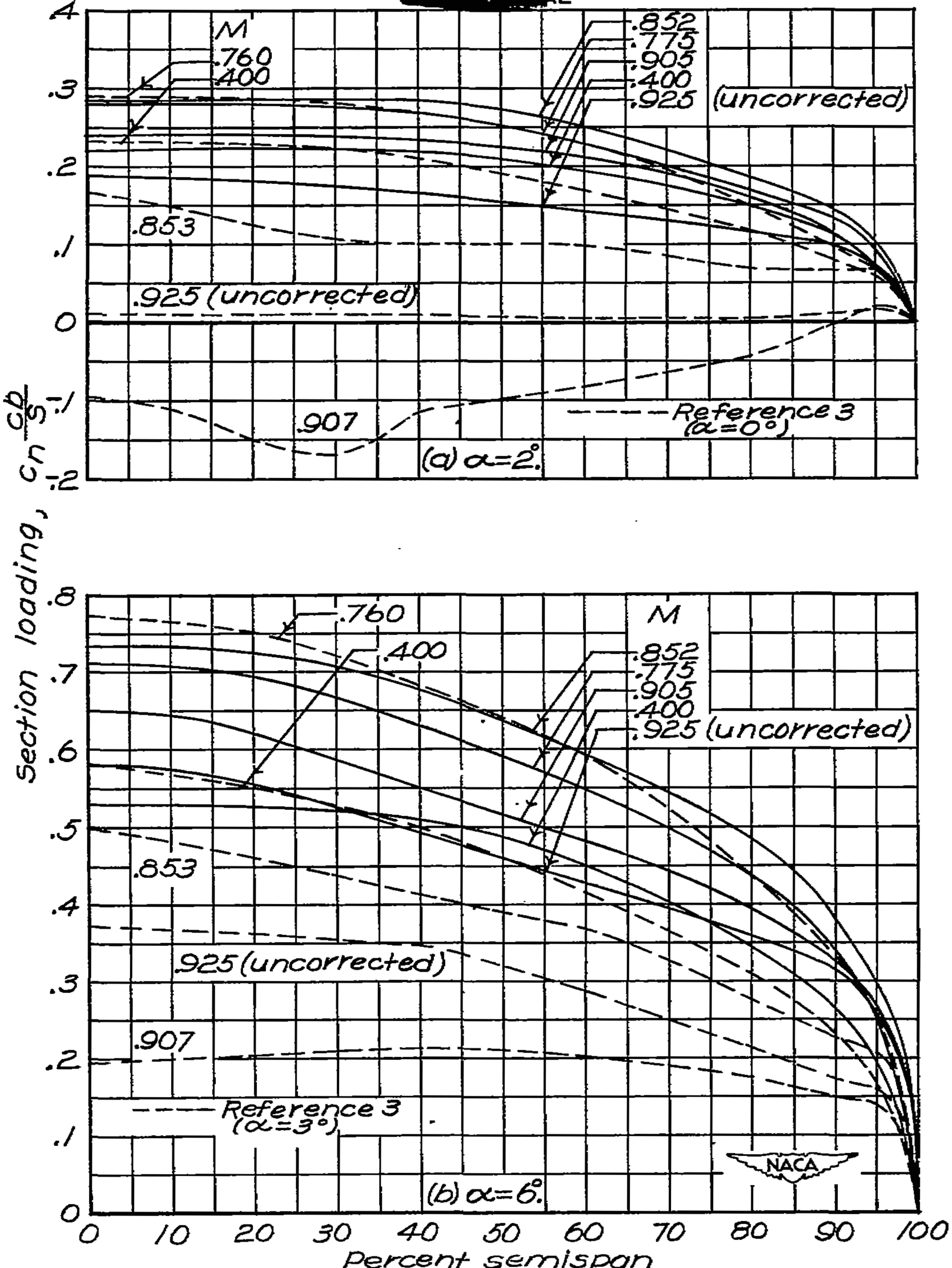

[redacted]

Figure 12.— Spanwise variation in section loadings.

[redacted]

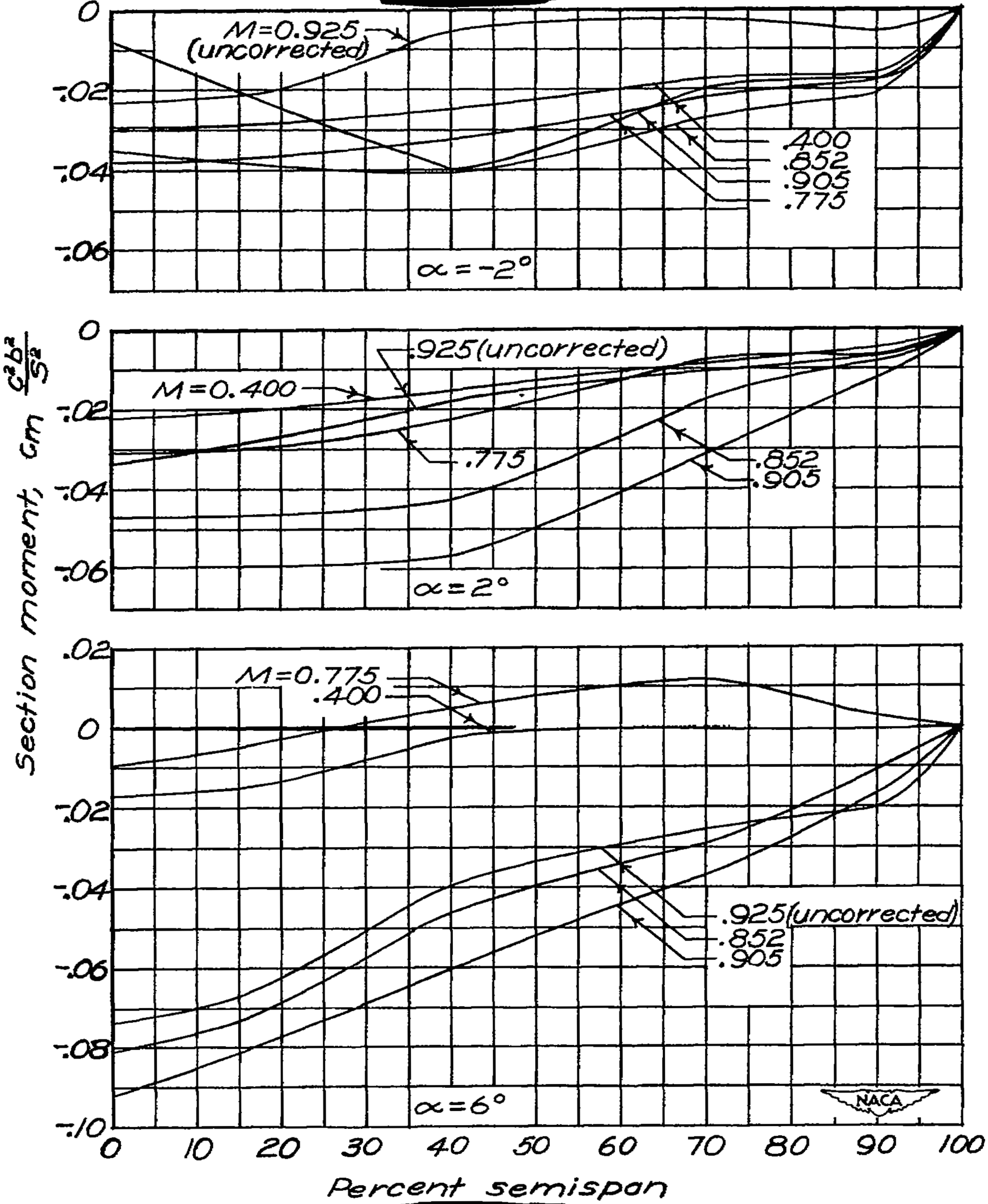

[redacted]

Figure 13.– Spanwise variation in section moment.

[redacted]

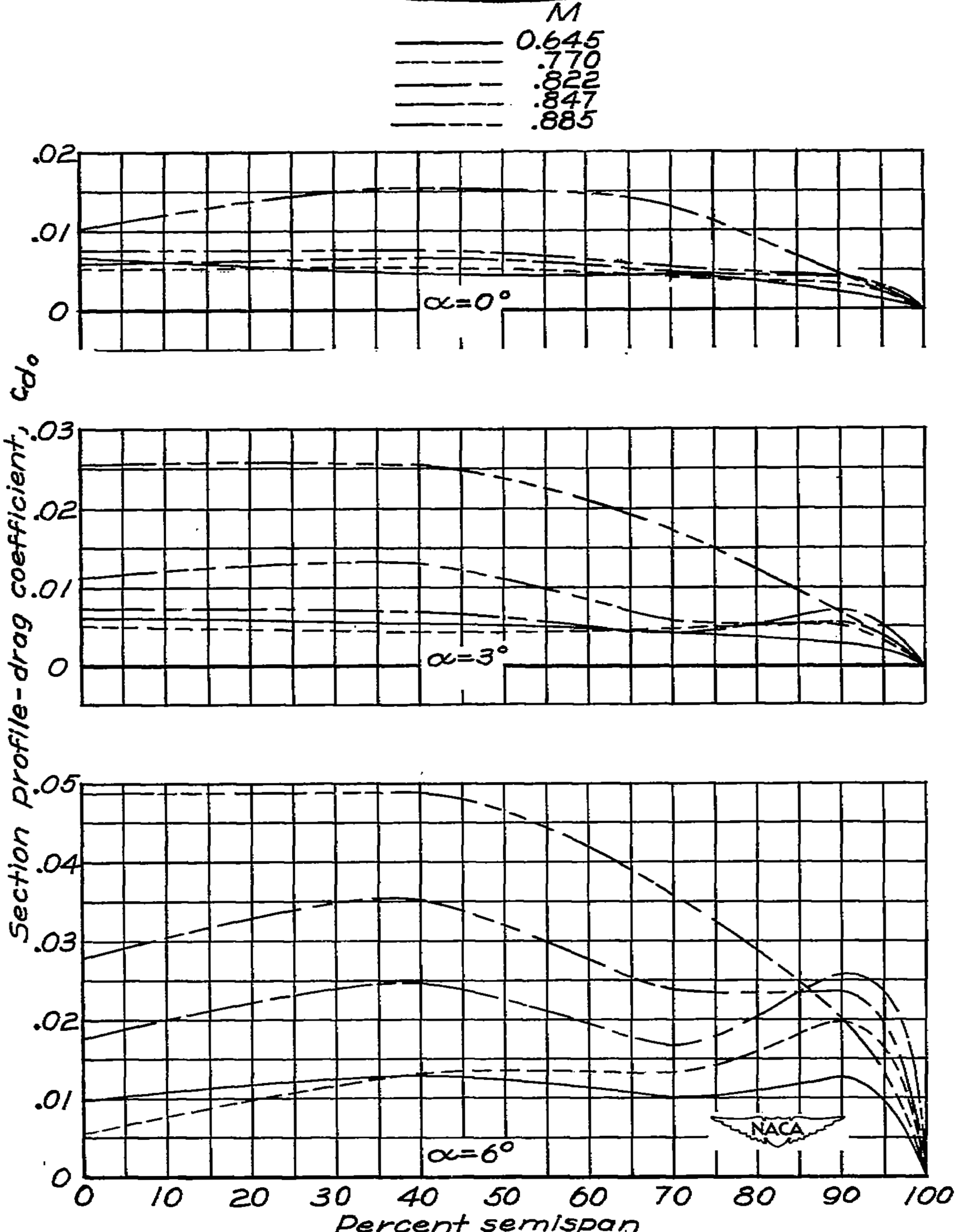

[redacted]

Figure 14.– Spanwise variation of section profile-drag coefficient.

[redacted]

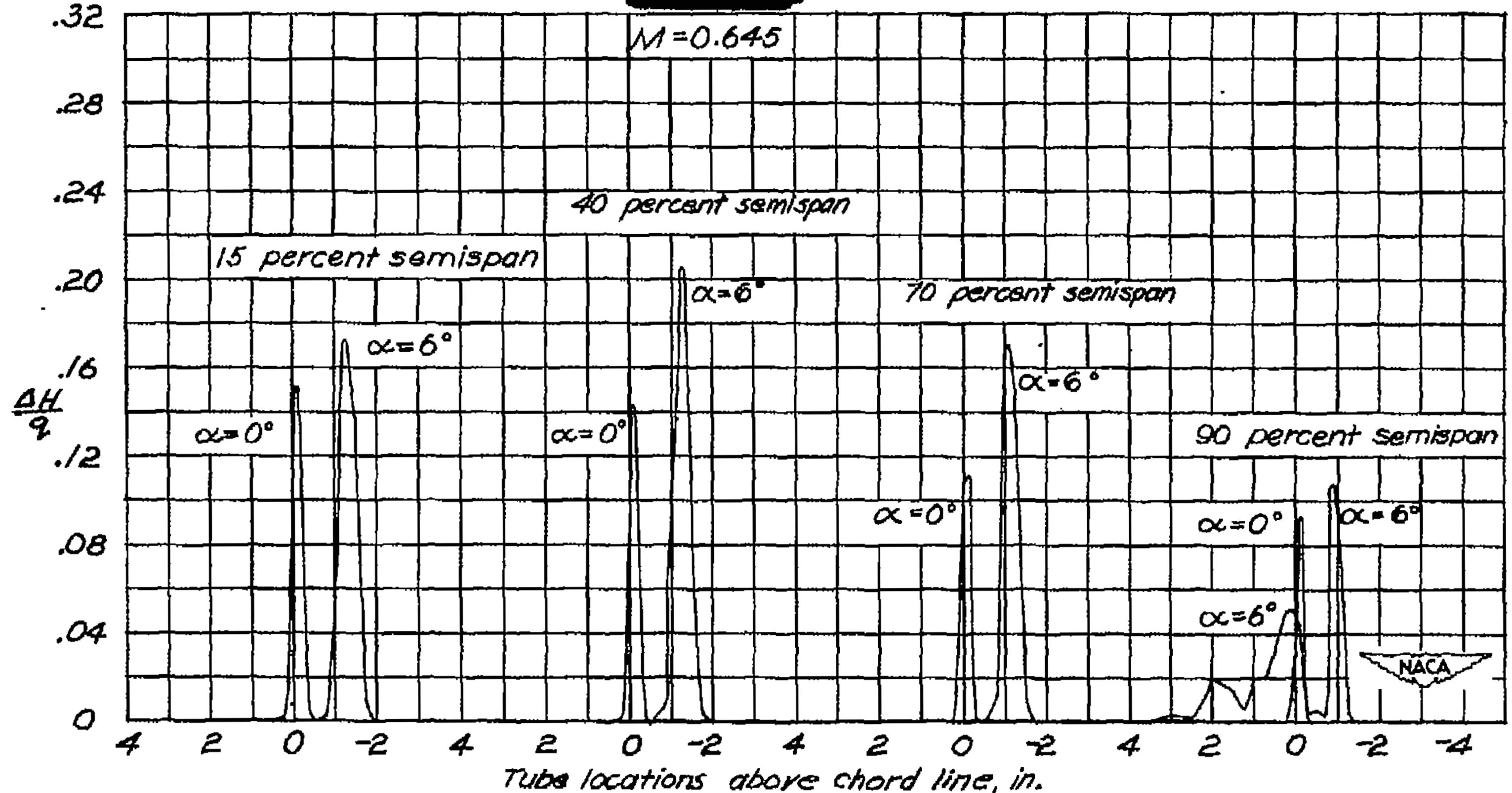

[redacted]

Figure 15.- Vertical variation of total-pressure losses at several spanwise stations 1.56 root chords behind the 70-percent-chord line.

[redacted]

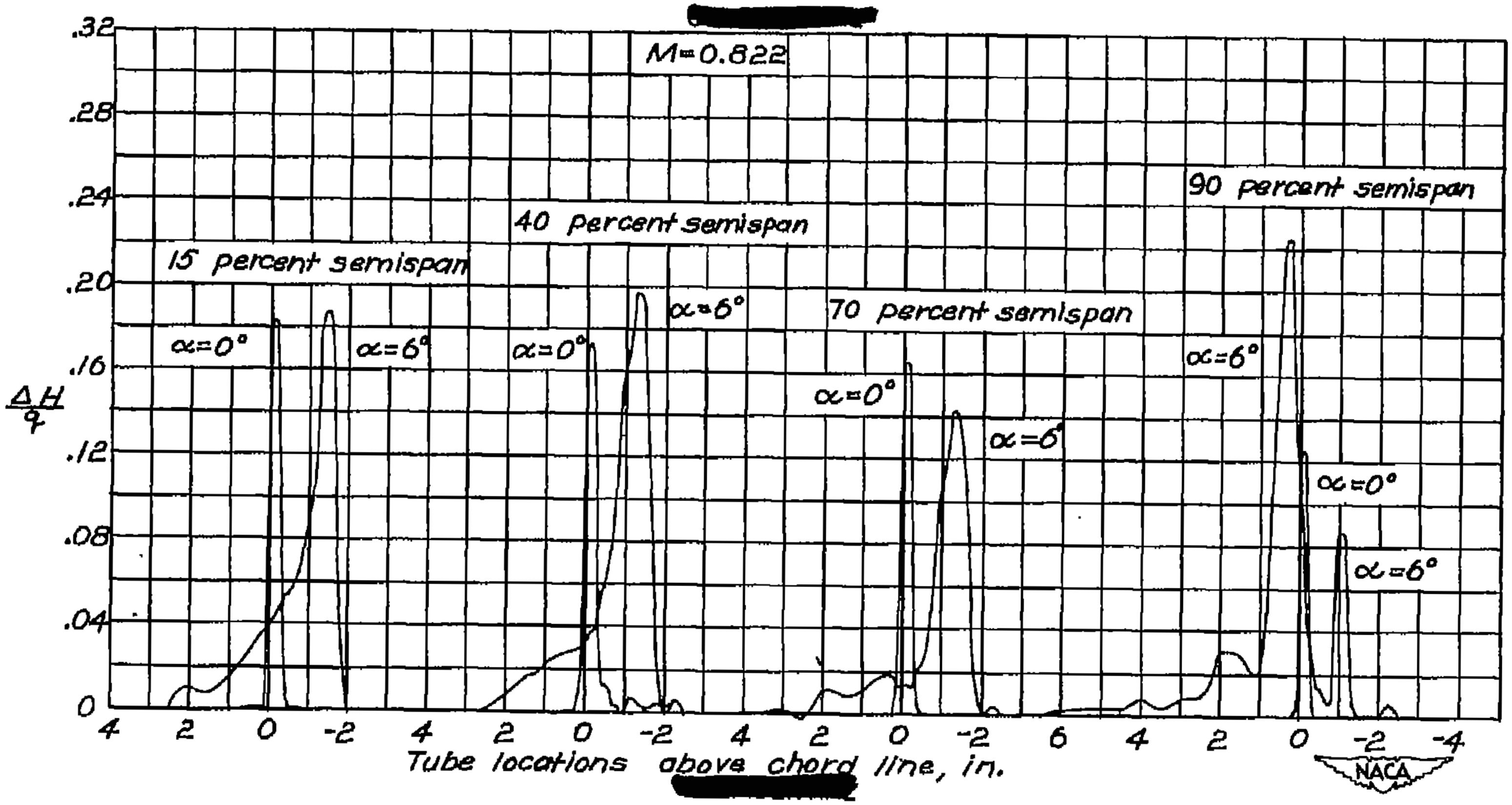

[redacted]

Figure 15.– Continued.

[redacted]

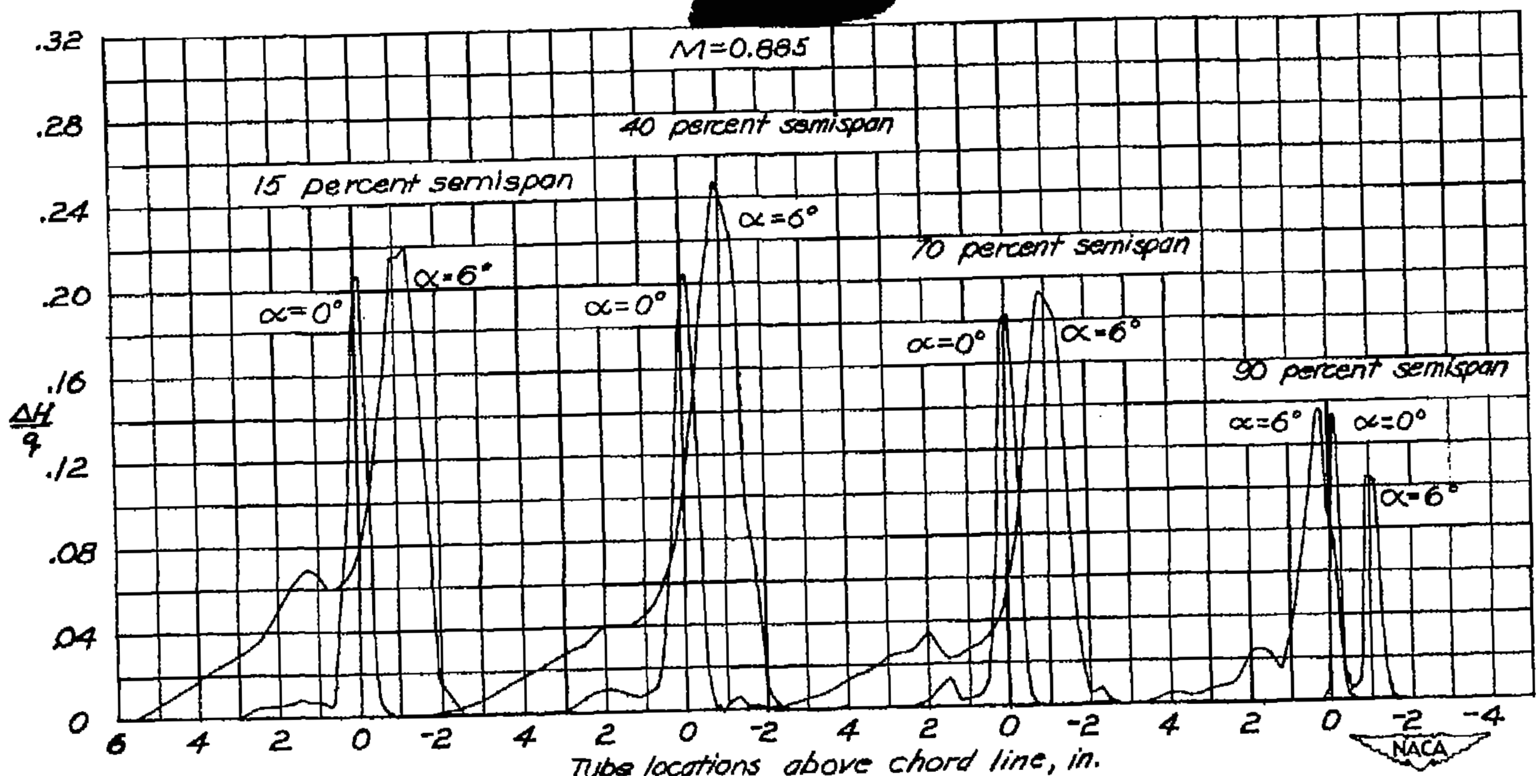

[redacted]

Figure 15.– Concluded.